Supporting information for:

Rhenium-Enhanced Cu nanowire catalyst for Efficient Electrocatalytic Hydrogenation of Furfural to Furfuryl Alcohol

Chen Chen [a], Changbao Zhou [a], Xiaotong Mu [a], Chenhao Yang [a], Hongke Li [a], Yiran Liu [a], Yao Chen [b,*] and Yunlei Zhang [a,*]

[a] Institute of Green Chemistry and Chemical Technology, School of Chemistry and Chemical Engineering, Jiangsu University, Zhenjiang212013, P. R. China

[b] School of the Environment and Safety, Jiangsu University, Zhenjiang212013, P. R. China

[*] Corresponding author Email: chenyao1390@ujs.edu.cn(Y.C.);jsdxzyl@ujs.edu.cn(Y.Z.)

1. Experimental section

1.1 Catalyst Characterizations

The X-ray diffraction (XRD) patterns were obtained on a Bruker D8 diffractometer using Cu Kα radiation. The scanning range was 10-80° with a scan speed of 7° min^{-1}. The images of samples were obtained by scanning electron microscope (SEM), transmission electron microscopy (TEM), and high-resolution TEM (HRTEM). The Brunauer–Emmett–Teller (BET) surface area of the materials was measured by N_2 adsorption-desorption isotherms at 77 K in an Autosorb-6B (Quantachrome Instruments). X-ray photoelectron spectroscopy (XPS) was measured by using a Thermo Fisher Scientific ESCALAB 250 with a monochromatized Al X-ray source. All XPS results were corrected by referencing the C1s speak at 284.8 eV. Electron spin resonance (ESR) spectra were recorded at room temperature on a Bruker E7407 spectrometer operating at X-band for radical intermediate detection. The HPLC analysis was performed using an Agilent Eclipse C18 column (250.0×4.6 mm, 5.0 μm) with UV-Vis and refractive index detectors (RID). The column temperature was set at 30 ℃ and the mobile phase consisted of a 0.1 wt% phosphoric acid and acetonitrile mixture at a 15:85 ratio. The flow rate was gradually increased from 0.2 mL/min to 1 mL/min, with the final pressure stabilizing around 197 bar.

1.2 Electrochemical measurements

All electrochemical tests were conducted in a 40 mL H-type three-electrode electrolytic cell, utilizing a cation exchange membrane. The electrolyte solution consisted of 1 M boric acid with a pH of 9.2. The prepared catalyst, a platinum electrode, and a mercury oxide electrode served as the working electrode, counter electrode, and reference electrode, respectively. The geometric surface area of the working electrode was 1 cm^2. For each electrocatalytic experiment, chronoamperometry

was employed, and all potentials were calibrated to the reversible hydrogen electrode (RHE) using Equation 1.

$$E_{RHE} = E_{(Hg/HgO)} + 0.0592 \times pH + 0.098 \#1$$

The E_{RHE} is the RHE after conversion, and the $E_{(Hg/HgO)}$ refers to the measured potential using the Hg/HgO electrode. The linear sweep voltammetry (LSV) was conducted at a scan rate of 5 mV/s, while cyclic voltammetry (CV) was performed at a scan rate of 100 mV/s. The electrochemical reduction of FF was carried out under magnetic stirring at 500 r min^{-1}. All experiments were carried out at room temperature and repeated three times to avoid standard errors.

1.3 In situ FTIR

The FTIR experiment was performed using a Thermo-Fisher Nicolet iS20, equipped with a liquid nitrogen-cooled MCT detector and a Si attenuated total reflection (UATR) accessory. The samples were cut into 0.5×0.5 cm^2 slices and immersed in a 50 mmol/L FF solution, with pH adjusted to 7.0 and a 0.5 M boric acid buffer. The working electrode was composed of the sample, while a platinum wire and Ag/AgCl electrode were used as the counter and reference electrodes, respectively. The spectral resolution was set to 8 cm^{-1}. Data collection was carried out simultaneously using the I-t technique at a potential of -0.65 V (vs. RHE) for 30 minutes. Prior to spectrum acquisition, the working electrode was pre-reduced at -0.65 V (vs. RHE) for 10 minutes to ensure the catalyst remained in a relatively stable state.

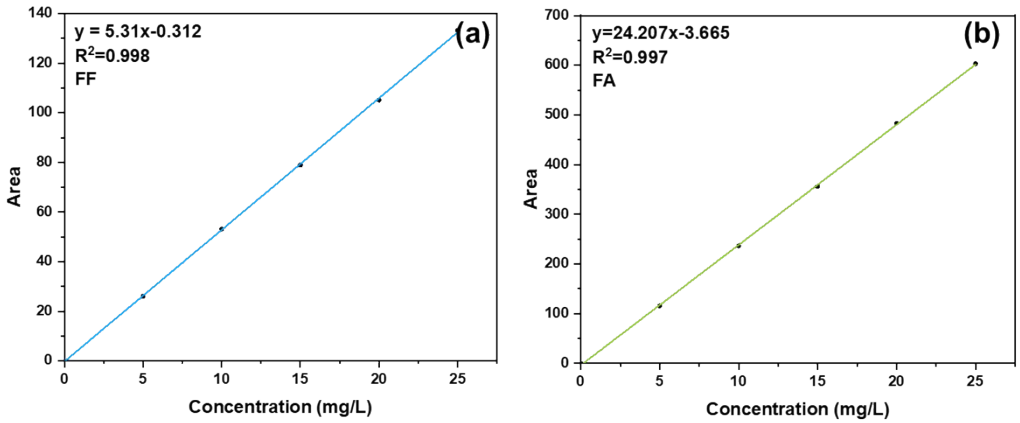

Figure S1. Standard curve of FF and FA.

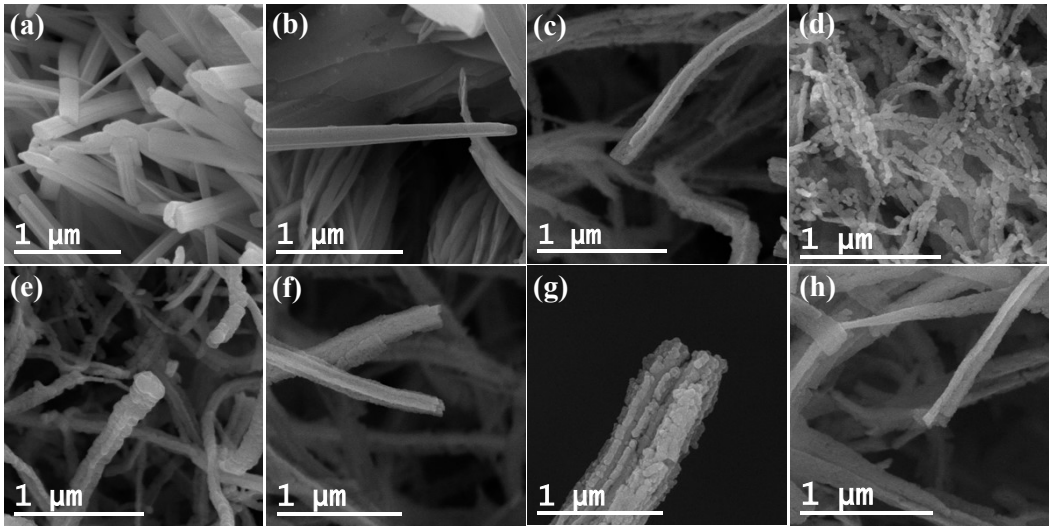

Figure S2. The SEM images of $Cu(OH)_2$ NW(a), CuO NW(b), Cu NW (c), $CuRe_{10}$ (d), $CuRe_{20}$ (e), $CuRe_{30}$ (f), $CuRe_{40}$ (g), $CuRe_{50}$ (h).

Figure S3. The EDS spectra of $CuRe_{40}$.

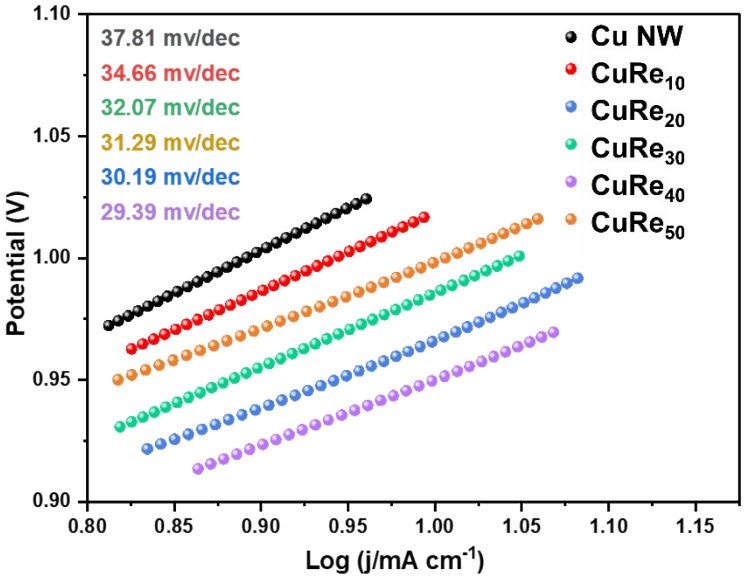

Figure S4. The Tafel slope of different samples.

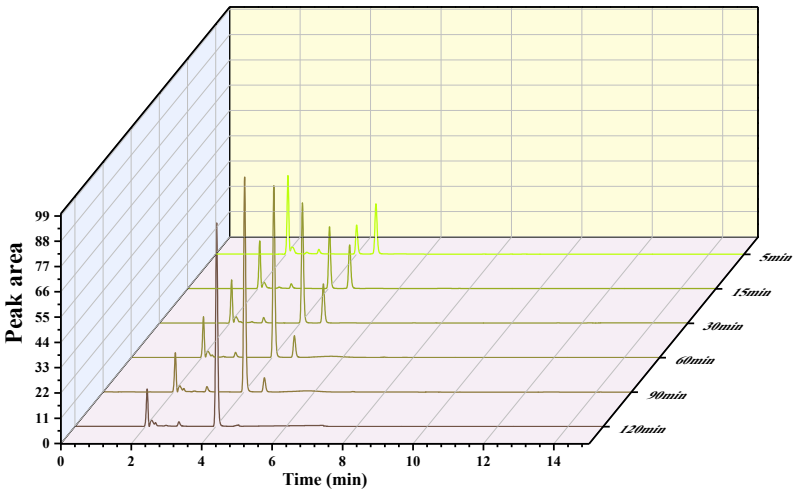

Figure S5. HPLC spectra of FF and FA.

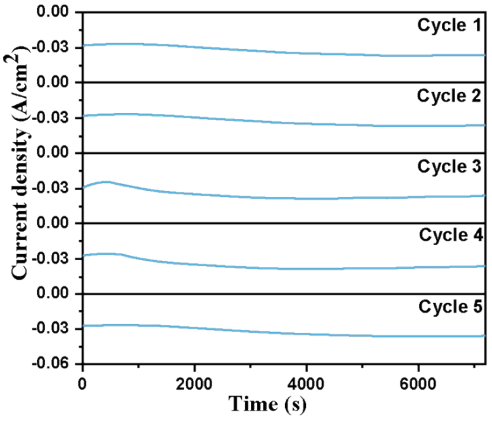

Figure S6. The I-t spectra in the regeneration experiment of $CuRe_{40}$.

Table S1. ICP result of Re NW/CF catalysts.

Catalysts	Cycles	Re-loading (mg)	Re-loading (wt %)
$CuRe_{10}$	10	0.8	0.72
$CuRe_{20}$	20	2.2	2.11
$CuRe_{30}$	30	3.5	3.37
$CuRe_{40}$	40	5.2	5.03
$CuRe_{50}$	50	6.8	6.42

Table S2. The S_{BET} value and average pore diameter of catalysts.

Catalysts	S_{BET} (m^2 g^{-1})	Average pore size (nm)
Cu NW	3.8208	12.848
$CuRe_{10}$	4.4292	9.5863
$CuRe_{20}$	4.6135	9.103
$CuRe_{30}$	4.7531	8.7463
$CuRe_{40}$	4.9023	8.6746
$CuRe_{50}$	5.3549	8.214

Table S3. FE, Conversion, and Yield of FA and FF at different pH over the $CuRe_{40}$ catalyst.

pH	F.E. (%)	Conversion (%)	Yield (%)
6.0	8	13	6
9.2	78	99	92
12.0	28	72	24

Table S4. FE, Conversion, and Yield of FA and FF at different potentials over the $CuRe_{40}$ catalyst.

Potential (V)	F.E. (%)	Conversion (%)	Yield (%)
1.1	63	69	61
1.2	78	99	92
1.3	45	99	82